Anal. Chem. **2004,** *76,* 796−804

A Model for the Quartz Crystal Microbalance Frequency Response to Wetting Characteristics of Corrugated Surfaces

Lisa A. Theisen* and Stephen J. Martin

Sandia National Laboratories, Albuquerque, New Mexico 87185

A. Robert Hillman

Department of Chemistry, University of Leicester, Leicester LE1 7RH, U.K.

We consider the effect of surface roughness, and its unique wetting behavior, on the response of a quartz crystal microbalance (QCM) resonator operating in contact with a fluid. The rough surface is modeled as sinusoidally corrugated particular to the case of a fixed relationship between amplitude and periodicity, as would arise from polishing with monodisperse spherical particles. The penetration of fluid into the troughs of the corrugations and the resulting meniscus are determined as a competition between surface tension and compression of the trapped gas. Liquid contained below the corrugation peaks, but above the gas/liquid meniscus, is trapped and behaves as an ideal mass layer, contributing a frequency shift that adds to that arising from liquid entrainment. This model allows QCM responses on rough surfaces to be described as a function of liquid properties and contact angle. This permits responses on hydrophobic surfaces to be understood in terms of incomplete surface wetting.

The quartz crystal microbalance (QCM) is one of a range of acoustic wave devices[1] that has been used to probe and characterize interfacial phenomena such as surface accumulation of material by adsorption/desorption or deposition/dissolution, surface roughness, viscoelasticity, stress, and interfacial slip.[2−11] Despite a considerable body of both theoretical and experimental literature, there are a number of experimental observations that are not presently explicable on the basis of the above listed phenomena. One notable absence from this list is interfacial wetting, which is widely appreciated and described in a substantial literature.[12−15] We therefore decided that it would be interesting to model the QCM response to this process.

Since interfacial de-wetting is known to occur at rough surfaces and the QCM is sensitive to fluid trapped in surface features ("roughness"), it therefore follows that the QCM will be sensitive to surface wetting or the absence thereof. This provided the motivation for us to model the wetting behavior of a corrugated surface exposed to different fluids and the resulting influence on QCM response. Given the number and diversity of processes to which the QCM responds (see above), a critical issue is the identification of conditions under which wetting behavior needs to be considered or indeed may be invoked as an explanation of recorded data.

Qualitative features of the QCM/fluid interaction are summarized in Figure 1. Figure 1a represents the entrainment of fluid by an oscillating smooth-surfaced QCM, as discussed by Kanazawa.[8] The oscillating surface generates a flow field $v_x(y,t)$ in the adjacent Newtonian liquid that varies with distance y from the surface and time t as

$$v_x(y,t) = v_{xo}e^{-y/\delta}\cos(y/\delta)\cos(\omega t) \qquad (1)$$

where v_{xo} is the amplitude of particle velocity at the QCM surface, $\omega = 2\pi f_s$, where f_s is the QCM series-resonant frequency and the decay length, δ, is given by[8]

$$\delta = (2\eta/\omega\rho)^{1/2} \qquad (2)$$

in which ρ and η are the liquid density and shear viscosity, respectively. According to eq 2, $\delta \approx 250$ nm for water in contact

* Corresponding author. E-mail: ltheise@sandia.gov. fax: 505-844-0011.

(1) Ballantine, D. S.; White, R. M.; Martin, S. J.; Ricco, A. J.; Zellers, E. T.; Frye, G. C.; Wohltjen, H. *Acoustic Wave Sensors: Theory, Design, and Physico-Chemical Applications*; Academic Press: San Diego, CA, 1997.
(2) Rodahl, M., Kasemo, B. *Sens. Actuators, A* **1996**, *54*, 448−456.
(3) Daikhin, L.; Urbakh, M. *Langmuir* **1996**, *12*, 6354−6360.
(4) Bandey, H.; Martin, S.; Cernosek, R.; Hillman, A. *Anal. Chem.* **1999**, *71*, 2205−2214.
(5) Ferrante, F.; Kipling, A. L.; Thompson, M. *J. Appl. Phys.* **1994**, *76*, 3448−3462.
(6) Schumacher, R. *Angew. Chem., Int. Ed. Engl.* **1990**, *29*, 329−343.
(7) Martin, S. J.; Granstaff, V. E.; Frye, G. C. *Anal. Chem.* **1991**, *63*, 2272−2281.
(8) Kanazawa, K. K.; Gordon, J. G. *Anal. Chem.* **1985**, *57*, 1770−1771.
(9) Yang, M.; Thompson, M. *Langmuir* **1993**, *9*, 1990−1994.
(10) Yang, M. S.; Thompson, M.; Duncan-Hewitt, W. C. *Langmuir* **1993**, *9*, 802−811.
(11) Martin, S. J.; Frye, G. C.; Ricco, A. J.; Senturia, S. D. *Anal. Chem.* **1993**, *65*, 2910−2922.
(12) Palasantzas, G.; de Hosson, J. T. M. *Acta Mater.* **2001**, *49*, 3533−3538.
(13) Nakae, H.; Inui, R.; Hirata, Y.; Saito, H. *Acta Mater.* **1998**, *46*, 2313−2318.
(14) Quere, D. *Physica A* **2002**, *313*, 32−46.
(15) Wapner, P.; Hoffman, W. *Langmuir* **2002**, *18*, 1225−1230.

10.1021/ac034777x CCC: $27.50
Published on Web 01/03/2004

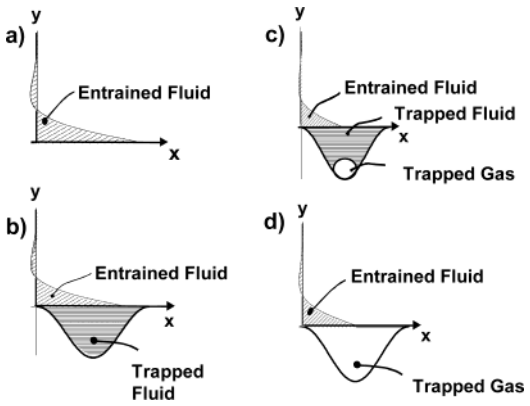

Figure 1. Schematic representations of viscously entrained fluid and trapped fluid at a surface that is (a) smooth, (b) rough and completely wetted, (c) rough and partially wetted, and (d) rough and completely de-wetted (no wetting).

with a 5-MHz QCM crystal; although there are obviously variations in δ with fluid properties and QCM device frequency, we shall see below that this provides an important benchmark for the scale of surface features. These mechanical effects resulting from the QCM/fluid interaction are transformed by the piezoelectric effect into an electrical response. This electrical response can be expressed through an equivalent-circuit model,[4,7,11] in which energy storage and dissipation, respectively, in the fluid are represented by an inductance and a resistance. These two circuit elements give rise, respectively, to a frequency shift, Δf, and damping of the resonance. The frequency shift for an *ideally smooth* surface (Figure 1a) is given by[7,8,16]

$$\Delta f \cong -\frac{f_s^{3/2}}{N}\left(\frac{\rho\eta}{\pi\mu_q\rho_q}\right)^{1/2} \qquad (3)$$

where N is the harmonic number of the resonance ($N = 1$ for all the data we will consider here), μ_q is the (piezoelectrically stiffened) quartz shear stiffness (2.947×10^{11} dyn/cm^2), ρ_q is the quartz mass density (2.651 g/cm^3), and f_s is the QCM base frequency.

The model described above applies to a "smooth" surface, where smooth implies that the dimension of surface features (represented later by h) is much smaller than the decay length in the fluid, i.e., h versus δ. Figure 1b represents the situation in which h is comparable to δ and there is complete wetting of the surface. This situation has been considered by Schumacher[6] and by Urbakh and Daikhin.[3,17−19] The simplest approach[6] is to assume that the lateral motion of surface features causes the incompressible trapped fluid to move synchronously with the crystal surface. The trapped fluid therefore behaves as an ideal mass layer: it generates an additional contribution to the frequency decrease, but no damping. The more sophisticated treatment of Daikhin et al.[20] takes into account the detailed structure of the surface features (distinguishing "slight" and "strong" roughness) and considers the relative sizes of the surface features and the fluid decay length. The trapped fluid now results in a contribution to *both* the frequency shift (decrease) *and* the damping of the resonator. Viscoelastic materials present in surface features behave in a fashion analogous to a fluid.[4]

The models considered by Schumacher,[6] Urbakh and Daikhin,[3,17−19] and Daikhin et al.[20] share two characteristics. First, the materials properties—viscosity for trapped fluid and shear modulus (G', G'') for viscoelastic materials—do not influence the QCM response; the amount of material (mass) is all that counts. Second, all these treatments are based on the notion that the surface features are *fully* filled. While this may be true in some cases, we recognize that it is simply one end of the spectrum of possibilities ranging from complete to zero filling. The extent of this filling will be determined by surface/fluid interfacial energetics.[21]

Our broad objective is to determine when, and to what extent, incomplete wetting of surface features significantly alters the QCM response. To achieve this, we calculate the profile of liquid penetration into surface features, integrate this to give the extent of fluid trapping, and calculate the resulting contribution to the QCM frequency response. The first two of these calculations involves surface/fluid interfacial characteristics (feature size and contact angle) and the third involves fluid characteristics (density). We then apply this unified model to data sets available in the literature. This new model will be shown to encompass both cases generally attributed to complete wetting and to provide a natural explanation for some other cases whose interpretation has been controversial.

THEORY

In this paper, we will model the surface roughness as a *sinusoidal corrugation* (as implied by Figure 1) with a single periodicity, Λ, and amplitude, A. This simplification ignores much of the complexity of a randomly rough surface but captures enough detail to explain many features observed with rough crystals. The relationship between Λ and A will be determined by the nature of the surface finishing process. For example, for a polishing process that uses monodisperse abrasive particles, a single periodicity will apply, and in the event that the particles are spherical, $A/\Lambda = {}^1/_4$.[22]

Complete Wetting Case. We first consider the case in which the corrugated surface is totally wetted and trapped fluid moves synchronously with the oscillating crystal surface. The total QCM response is the sum of the Kanazawa expression and a gravimetric term obtained by applying the Sauerbrey equation[23] to the aerial mass density of entrapped fluid. This total frequency shift for a *completely wetted* corrugated (more generally rough) surface can be written

(16) Reed, C. E.; Kanazawa, K. K.; Kaufman, J. H. *J. Appl. Phys.* **1990**, *68*, 1993−2001.
(17) Urbakh, M.; Daikhin, L. *Langmuir* **1994**, *10*, 2836−2841.
(18) Urbakh, M.; Daikhin, L. *Phys. Rev. B* **1994**, *49*, 4866−4870.
(19) Urbakh, M.; Daikhin, L. *Colloids Surf., A* **1998**, *134*, 75−84.
(20) Daikhin, L.; Gileadi, E.; Katz, G.; Tsionsky, V.; Urbakh, M.; Zagidulin, D. *Anal. Chem.* **2002**, *74*, 554−561.
(21) Adamson, A. W. *Physical Chemistry of Surfaces*, 5th ed.; Wiley: New York, 1990.
(22) Polishing with spherical abrasive particles produces surface channels that we approximate as sinusoidal with depth 2A equal to full width at half-height ($\Lambda/2$). This results in a fixed relationship between amplitude A and periodicity Λ: $A/\Lambda = 1/4$.
(23) Sauerbrey, G. Z. *Phys.* **1959**, *155*, 206−222.

$$\Delta f = -\frac{f_s^{\,2}}{N(\rho_q\mu_q)^{1/2}}\left(\frac{\rho\eta}{\pi f_s}\right)^{1/2}\left[1+\pi\left(\frac{h}{\delta}\right)\right] \qquad (4)$$

where h is defined as the *average vertical deflection about the mean* (corresponding to how roughness will be quantified,[11] and one can show that $h = (2/\pi)A$).

When $h/\delta \ll 1$, the bracketed term in eq 4 reduces to unity, and the Kanazawa result is obtained; from the perspective of the QCM, this constraint on h defines a "smooth" surface. Physically, this corresponds to dominance of viscous entrainment over fluid trapping (Figure 1a), in which case the frequency shift is proportional to $(\rho\eta)^{1/2}$.

When h is comparable to δ (Figure 1b), then trapping of fluid contributes significantly to the QCM response. We can recast eq 4, for the *completely wetted* corrugated surface, as

$$-\frac{\Delta f}{\rho} = \frac{f_s^{\,3/2}}{N(\rho_q\mu_q\pi)^{1/2}}\left(\frac{\eta}{\rho}\right)^{1/2} + \frac{\pi f_s^{\,2}h}{N(\rho_q\mu_q)^{1/2}} \qquad (5)$$

This relationship provides a means for extracting h, based on fitting (by linear regression) the frequency response $(\Delta f/\rho)$ of a given resonator in a series of fluids of different $(\eta/\rho)^{1/2}$.

Incomplete Wetting Case. There are a number of reports indicating that trapped gas has been observed at the interface between a rough surface and a contacting fluid.[24,25] For the purposes of illustration, we will suggest one means by which a gas (air) could be trapped at the solid/liquid interface. However, since the arguments we shall develop are based on equilibrium concepts, the mechanism and rate of achieving this physical situation are immaterial. Further, since all noncondensed phases will give effectively zero coupling to the resonator (as compared to a condensed phase), the identity of the gas—air, gas previously trapped in the solid, or vapor from the liquid (according to the vapor pressure appropriate to the experimental temperature)—is unimportant.

In the model, resonator immersion and resultant trapping of gas can be envisaged via the following sequence of events. When liquid first contacts the sinusoidally corrugated surface,[26] it "sheets" over the surface, contacting only the peaks of surface features. Liquid then enters the troughs of the corrugations, compressing the trapped gas into microbubbles at the bottoms of the troughs.[27,28] The extent of the liquid penetration (wetting) of the microscopic surface features is strongly influenced by the surface roughness[12,26,28] and the (microscopic) liquid contact angle, θ[28] (see Figure 2). Qualitatively, the more lyophobic the surface, the greater the contact angle and the less complete the wetting of the surface features (here modeled as sinusoidal corrugations).

The meniscus shape is determined by a balance of two pressures, arising from surface tension, γ, $(P_1 = \gamma/r)$ and from internal gas pressure (P_2), as schematically illustrated in Figure 2. In the model developed above, the amount of trapped gas is determined by the initial (ambient) pressure and the volume of the surface feature. Under the constraint that gas initially trapped in surface features is retained there, the final pressure is given by $P_2 = P_0(\mathcal{A}_1/\mathcal{A}_2 - 1)$, where P_0 is the ambient air pressure and $\mathcal{A}_1$ and $\mathcal{A}_2$, respectively, are the cross-sectional areas in the absence and presence of gas compression in the surface corrugations (see Figure 2). Relaxation of this constraint, allowing entry or exit of gas from the cavity, would lead to a new meniscus. Although a different number of moles of gas would be present, the same requirement of balanced surface tension and compression forces $(P_1 = P_2)$ would apply. The most extreme case would be complete dissolution of the air and replacement by solvent vapor. In this case, P_2 would be given by the vapor pressure of the solvent.

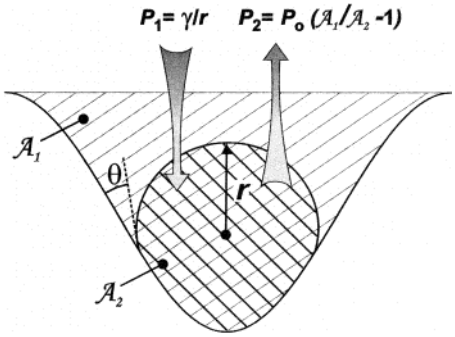

Figure 2. Schematic illustration of the geometry and pressures determining the shape of a trapped gas bubble within a sinusoidal corrugated surface feature.

For large surface features, i.e., Λ greater than a few hundred nanometers, the two models (either fixed trapped gas or allowing dissolution) described in the previous paragraph predict substantial differences in fluid penetration and consequent QCM frequency response. The result would be an initial response given by the first model, followed by a transient approach to the second model. The time scale of this transient would be governed by solution mass transport processes and gas solubility. However, for smaller surface features, $\Lambda \approx 100$ nm—the situation of practical interest—the two models give very similar results.

Based on the fixed trapped gas model (but bearing in mind the relative insensitivity to model for the conditions of interest), we are able (see Supporting Information) to predict the wetting behavior. Figure 3 illustrates the results for a range of experimentally accessible conditions (surface corrugation periodicity and microscopic contact angle). In each case, we have defined the aspect ratio of the surface features by setting $A/\Lambda = {}^1/_4$, corresponding to the common practice of preparing a surface by polishing with spherical abrasive particles. Within Figure 3, at fixed corrugation size, we examine the effect of microscopic contact angle. Qualitatively, we see that, as contact angle increases, liquid penetration decreases. In Figure 3, we see that decreasing feature size increases the sharpness of the transition between complete wetting and substantial fluid exclusion. This is a consequence of the fact that P_2 is based on the bubble *volume*, while P_1 is based on bubble *surface area*. Quantitatively, the wetting characteristics can be illustrated by two numerical comparisons, exploring the effects of contact angle and corrugation periodicity, respectively. First, at a constant contact angle of

(24) Lubetkin, S. D. *Chem. Soc. Rev.* **1995**, *24*, 243−250.
(25) Lubetkin, S. D. *Langmuir* **2003**, *19*, 2575−2587.
(26) Peng, M.; Kurokawa, T.; Gong, J.; Osada, Y.; Zheng, Q. *J. Phys. Chem. B* **2002**, *106*, 3073−3081.
(27) Jones, S. F.; Evans, G. M.; Galvin, K. P. *Adv. Colloid Interface Sci.* **1999**, *80*, 27−50.
(28) Bankoff, S. G. *AICHE J.* **1958**, *4*, 24−26.

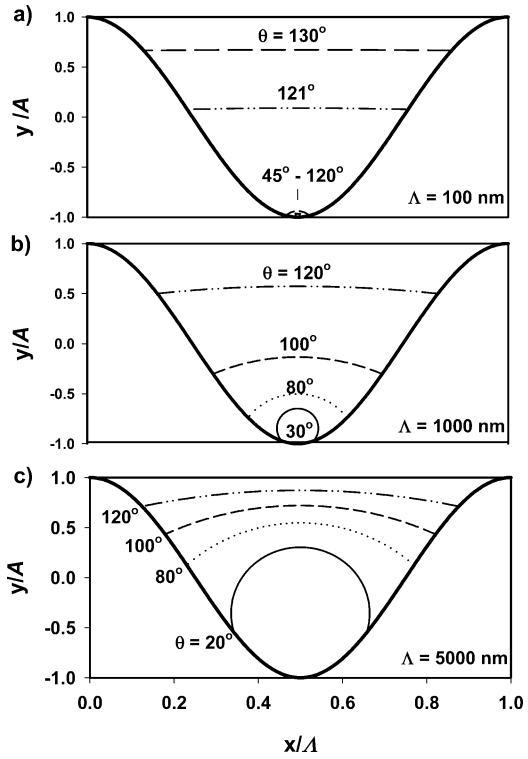

Figure 3. Wetting of a rough (sinusoidally corrugated) surface illustrating calculated bubble size according to the Supporting Information, as a function of microscopic liquid contact angle (θ). Surface feature sizes (Λ): (a) 100, (b) 1000, and (c) 5000 nm (A/Λ = 1/4 in all cases). Contact angle is as indicated.

$\theta = 60°$, the meniscus pressure is 1.2×10^9, 9.6×10^6, and 5.7×10^5 dyn/cm^2 (i.e., approximately 1200, 10, and 0.6 atm) for Λ = 100, 1000, and 5000 nm, respectively (the corrugations in Figure 3).

The result—graphically illustrated in Figure 3—is complete, virtually complete, and only moderate filling of the corrugation with liquid, respectively. Second, focusing on the surface corrugation and taking the practically relevant case of Λ = 100 nm (Figure 3a), the corrugation remains virtually filled with liquid when $\theta < 120°$ but empties rapidly as θ exceeds 120°; an increase of just a few degrees effects the transition. Rejmer et al. predicted a similar abrupt emptying of a wedge-shaped surface feature at $\theta = 120°$ when the length scale is on the order of 100 nm.[29] For Λ = 1000 nm (Figure 3b), the corrugation empties more gradually over the range $30° < \theta < 120°$. At the largest corrugation size considered, Λ = 5000 nm (Figure 3c), the corrugation never completely fills because capillary forces are insufficient to counteract the bubble's gas pressure. (Although the "fixed trapped gas" model is arguably less applicable here in practice, the qualitative conclusion is unaltered.)

The meniscus shape data illustrated in Figure 3 allow us to calculate the volume of trapped gas. By subtraction from the total cavity volume, one can readily calculate the volume (fraction) of liquid present in the surface corrugations. Representative calculations, using values from Figure 3 and analogues for other Λ values, are shown in Figure 4. The sharpness of the wetting/de-wetting transition, as contact angle is varied, for small surface features is

(29) Rejmer, K.; Dietrich, S.; Napiorkowski, M. *Phys. Rev. E* **1999**, *60*, 4027–4042.

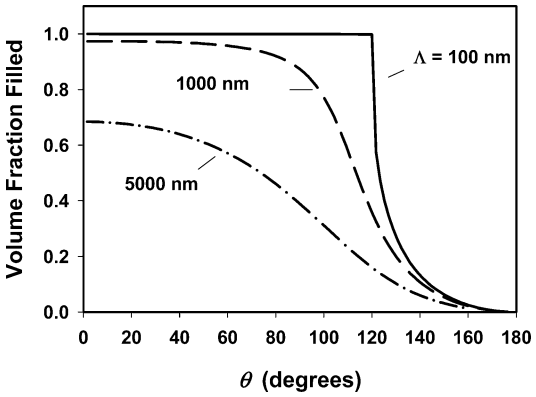

Figure 4. Calculated volume fraction filled by liquid, $(\mathcal{A}_1 - \mathcal{A}_2)/\mathcal{A}_1$ as a function of contact angle (θ), for different corrugation sizes (Λ).

dramatically highlighted. We note, from Figure 4, that in the wetting scenario considered, complete filling of features *never occurs* even under the most hydrophilic surface condition: $\theta \rightarrow 0$. (We note, however, that the circular bubble assumption breaks down for sufficiently large features.) The remaining trapped air bubble excludes some fraction of liquid, $\mathcal{A}_2/\mathcal{A}_1$. Thus, eq 5, based on total filling of the corrugation, is in error by an amount equal to this bubble fraction. The present analysis indicates a bubble fraction (error in eq 5) at maximum filling (for $\theta \rightarrow 0$) of 3×10^{-4} for Λ = 100 nm, 0.026 for Λ = 1000 nm, and 0.32 for Λ = 5000 nm. Thus, for small features ($h \leq 100$ nm) and low contact angle, the approximation of total filling is good; this degrades as feature size or contact angle increases.

QCM Response. The results of the previous section now allow us to proceed directly to a prediction of the QCM frequency response, i.e., the change in resonant frequency (Δf) due to liquid loading. Although we do so for a range of surface roughness conditions, we emphasize that the most dramatic and practically relevant effects are for the case in which roughness features are small compared with the liquid decay length ($h/\delta \leq 1$; see Figure 1a and relevant components of Figure 3 and Figure 4). Consistent with the constraint applied to the fully filled corrugation case,[6] we assume that any liquid *below* the peaks of the surface features moves synchronously with the oscillating QCM surface. Since corrugation-entrapped fluid—regardless of the extent of filling—moves synchronously with the resonator, the viscous entrainment of fluid *above* the peaks is identical in all cases. The entrapped fluid behaves as an ideal mass layer and, adding to the contribution from entrained fluid, contributes a frequency shift for the *partially wetted* corrugated surface:

$$-\frac{\Delta f}{\rho} = \frac{2f_s^2}{N(\rho_q \mu_q)^{1/2}}\left[\frac{\mathcal{A}_1 - \mathcal{A}_2(\theta)}{\Lambda} + \frac{\delta(\eta,\rho)}{2}\right] \qquad (6)$$

where $\mathcal{A}_1 = A\Lambda = \Lambda^2/4$; the Supporting Information describes the calculation of $\mathcal{A}_2(\theta)$; $\delta(\eta,\rho)$ is the liquid decay length, given by eq 2. In the regime of corrugation size and contact angle where nearly complete filling occurs, $\mathcal{A}_2 \rightarrow 0$ and eq 6 reduces to eq 5.

Figure 5 shows the frequency shift, based on eq 6, versus contact angle for several corrugation sizes, all with $A/\Lambda = 1/4$. At low contact angle, where the most filling occurs, the frequency shift increases with feature size, Λ; this limiting case corresponds

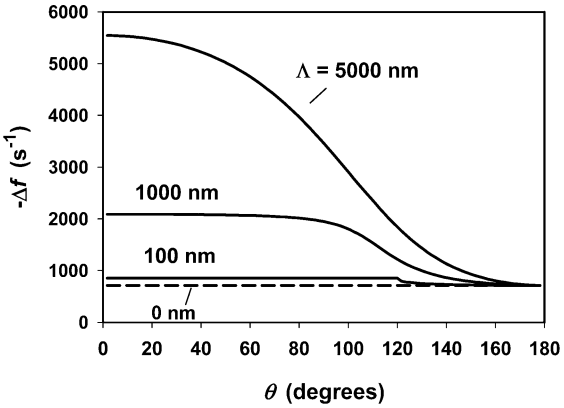

Figure 5. Calculated QCM frequency shift ($-\Delta f$) as a function of contact angle (θ) for sinusoidally corrugated surfaces immersed in water at 20 °C with $A/\Lambda = 1/4$; QCM base frequency (f_s), 5 MHz.

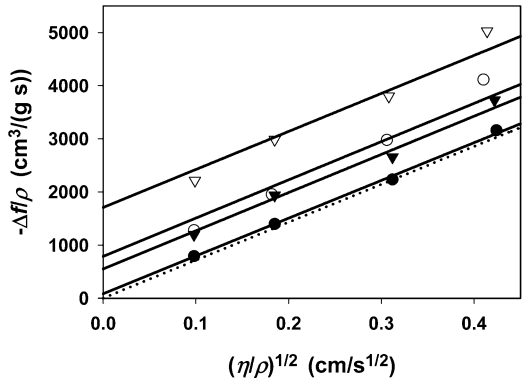

Figure 6. Normalized frequency shift ($-\Delta f/\rho$) vs fluid properties ($(\eta/\rho)^{1/2}$) for glycerol/water mixtures on QCMs of different roughnesses (●, $h = 9.5$ nm; ▼, $h = 62$ nm; ○, $h = 89$ nm; ▽, $h = 192$ nm).[11] Lines are calculated best fits of eq 5 using surface roughness (h) as a parameter (values are listed in Table 1, along with optical and profilometer roughness measurements for comparison). Dashed line is predicted from the simple (Kanazawa) model (eq 3) that assumes an ideal smooth surface ($h = 0$).

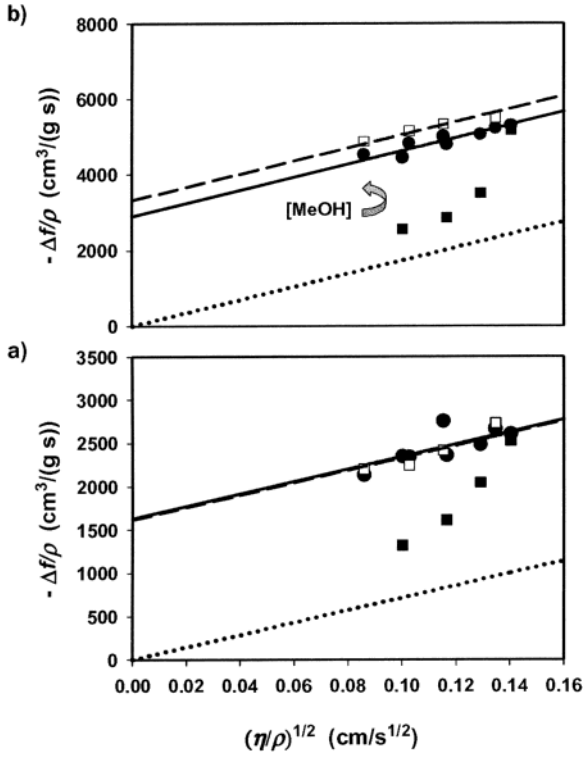

Figure 7. Normalized frequency shift ($-\Delta f/\rho$) vs fluid properties ($(\eta/\rho)^{1/2}$) for different MeOH/water solutions[10] on uncoated and HDM-coated QCMs: (a) 5-MHz device; (b) 9-MHz device. Data for the uncoated QCM (●) and data for the HDM-coated QCM (□ and ■). Dotted line is calculated from simple (Kanazawa) model (eq 3) for an ideal smooth surface. Other lines are best fits of eq 5 (solid line is the best fit to uncoated QCMs and dash line is best fit to the HDM-coated) QCMs to the data (■ data not used) to extract surface roughness (h), listed in Table 2.

to eq 5. As contact angle increases, liquid is progressively excluded and eventually all the curves asymptote to the Kanazawa result: since the features are unfilled, their size is irrelevant.

Our new model predicts the frequency shift resulting from liquid loading, accounting for changes in interfacial wetting. The contact angle variations that lead to these changes may be associated with substantial changes in bulk fluid properties (viscosity, density) in the case of mixed fluids, or they may be essentially independent of bulk fluid properties in the case of added surfactants. The significance of independent variation of θ and η/ρ will become clear later in the paper.

RESULTS AND DISCUSSION

Results. We show (see Figure 6 and Figure 7) two sets of data taken from the literature for QCM responses to immersion in different fluids. In both cases, the observed frequency changes accompanying fluid immersion are significantly different from the predictions of the Kanazawa model (eq 3; Figure 1a). In such cases, the first line of enquiry is to explore the possibility that simple roughness arguments with complete wetting (Figure 1b) can explain these effects. Hence, we plot the data according to the form of eq 5, i.e., $-\Delta f/\rho$ versus $(\eta/\rho)^{1/2}$. The slope of such a plot (varying fluid properties) should depend only on crystal properties and the intercept on crystal properties and surface feature size (h).

Figure 6 shows frequency response data for a 5-MHz AT-cut resonator immersed in a series of glycerol/water mixtures.[11] We plot the data according to the form of eq 5, since this allows separation of the fluid and resonator characteristics. For a given crystal, varying fluid composition alters (η/ρ) and thus δ (see eq 2), thereby resulting in variation in the entrained fluid mass (see Figure 1a). Since the mass of trapped fluid is determined by the product ρh, exposing a series of crystals of varying roughness (all represented by Figure 1b) to the same sequence of fluids should generate a set of parallel lines, the slopes of which correspond to the Kanazawa (smooth surface) result. This is exactly what we find in Figure 6.

The intercepts on the $-\Delta f/\rho$ axis, were collected as extracted h values in Table 1 and represent the resonator surface roughness.[30] These h values are compared in Table 1 with two independent measures of surface roughness obtained using optical and mechanical devices (a Wyko RST profiler and a Dektak Profilometer, respectively). When $h/\delta \leq 0.5$, the QCM-derived roughness value (h) is comparable to the roughness measurements extracted from optical and profilometer measurements.

(30) We have assumed total wetting. For feature sizes $h \leq 500$ nm, $A_2/A_1 \leq 0.007$, giving an estimate of the error arising from this assumption.

Table 1. Comparison of QCM Surface Roughness Values (h) (Data from Figure 6)[11]

symbols in Figure 6	QCM[a] h (nm)	Profilometer[b] h_1 (nm)	optical[c] h_2 (nm)	h_2/δ[d]
●	9.5	3	<10	<0.04
▼	62	102	197	0.79
○	89	68	156	0.62
▽	192	445	525	2.1

[a] Obtained by fitting data of Figure 6 to eq 5. [b] Obtained using Dektak model IIA profilometer, in which a contacting diamond stylus (12.5-μm radius; 2g force) measured a single-line profile across the surface, from which the average surface roughness is calculated. Slow scan speed; scan length of 1 mm; vertical resolution ~0.1 nm; lateral resolution limited by stylus radius to a few microns. [c] Obtained using Wyko RST profiler, in which a vertical-scanning interference microscope yields a noncontacting two-dimensional surface profile. Scanned area 100 μm^2; measurement range 10 nm to 100 μm; vertical resolution 3 nm; lateral resolution ~0.5 μm. [d] δ = 250 nm.

The different surface roughness probes show quantitative differences as a consequence of their reliance upon different phenomena, their response on different (or differently weighted) length scales, and the sampled area of surface. We do not dwell on the details of this issue,which has been observed previously.[31,32] We simply note that the qualitative level of agreement is a measure of the acceptability of the ideal (single characteristic length and geometry) model we employ with its considerable advantages of algebraic tractability.

We note that the simple model in Figure 6 (eq 3; dashed line) works when $h/\delta \ll 1$. When h/δ is no longer negligible, the corrugated surface model accounts for the additional frequency shift caused by fluid trapping in roughness features. For $h/\delta >$ 1, the QCM-derived h value is significantly smaller than the other determinations. In this regime, the acoustic decay across the liquid within the corrugation channel becomes significant; i.e., only a part of the trapped fluid is acoustically coupled and thereby sensed so the simple "gravimetric" picture of complete liquid trapping below the peaks is inadequate.

The second example, shown in Figure 7 and again plotted in the format of eq 5, contains four sets of experiments[10] involving AT-cut crystals of base frequency 5 and 9 MHz, each uncoated ("*bare*") and following a hexadecyl mercaptan (HDM) hydrophobic surface treatment ("*coated*"). In each case, the crystal was immersed in a series of H_2O/MeOH solutions, thereby varying $(\eta/\rho)^{1/2}$. The two sets of data for the *uncoated* crystals (● in Figure 7) follow the pattern predicted by eq 5: the $-\Delta f/\rho$ values increase linearly with $(\eta/\rho)^{1/2}$, at a rate (slope) consistent with the Kanazawa model (eq 3). The intercepts as $(\eta/\rho)^{1/2} \rightarrow 0$ of the two plots yield the roughness parameters listed in Table 2. In each case, $h < \delta$, so the bounds of the simple fluid entrapment model are not exceeded.

Turning to the *coated* (hydrophobic) crystal responses (□, ■ in Figure 7), the picture is somewhat more complex. At high MeOH concentrations, (□), the data conform to the model developed for the "bare" crystals. Specifically, the slopes follow the Kanazawa model and the derived roughness parameters (h in Table 2) are the same, within experimental uncertainty, as those for the *uncoated* surfaces. (To the extent that the thickness of the hydrophobic coating is much less than h, this is a requirement of any physically reasonable model.) However, at low MeOH concentrations, (■), the $-\Delta f/\rho$ values depart significantly from the roughness-enhanced Kanazawa values and in fact approach the dotted line calculated for an ideal smooth surface (■ data points were not used for h determination in Table 2). The unequivocal conclusion is that the fully wetted corrugated surface model (see Figure 1b) is inadequate to describe these data. We therefore now investigate whether the decreased $-\Delta f$ values at low MeOH concentrations (■) can be explained by incomplete wetting of the surface features, as illustrated in Figure 1c,d.

Table 2. QCM Surface Roughness Parameter (h) (Extracted from Data of Figure 7)[10]

	5-MHz device	9-MHz device
h (uncoated) (nm)	182	115
h (HDM-coated) (nm)	190[a]	101[a]

[a] Low MeOH fraction values (■) were not used in h determination.

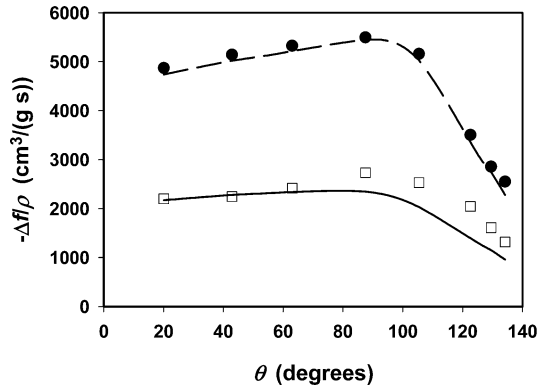

Figure 8. Normalized frequency shift ($-\Delta f/\rho$) vs contact angle (θ) for different MeOH/H_2O solutions.[10] Data for the 5-MHz HDM-coated QCM (□) and the 9-MHz HDM-coated QCM (●). The lines are calculated from the partial wetting model at 5 and 9 MHz.

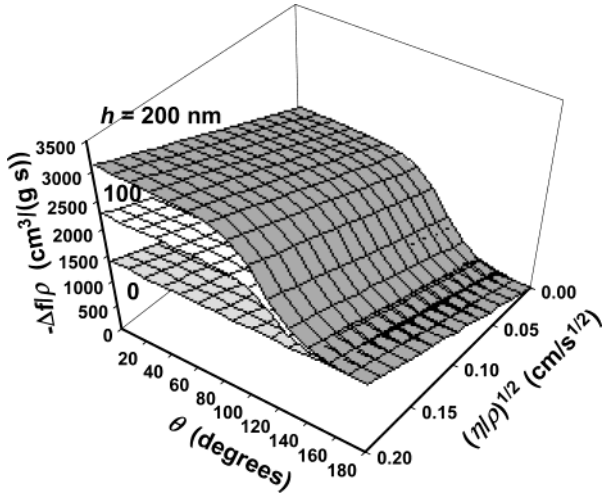

Figure 9. 3D plot of calculated normalized frequency shift ($-\Delta f/\rho$) vs fluid properties ($(\eta/\rho)^{1/2}$) and contact angle (θ) for (f_s = 5 MHz) and h = 0, 100, and 200 nm.

(31) Rudich, Y.; Benjamin, I.; Naaman, R.; Thomas, E.; Trakhtenberg, S.; Ussyshkin, R. *J Phys. Chem. A* **2000**, *104*, 5238−5245.

(32) Stalgren, J.; Eriksson, J.; Boschkova, K. *J. Colloid Interface Sci.* **2002**, *253*, 190−195.

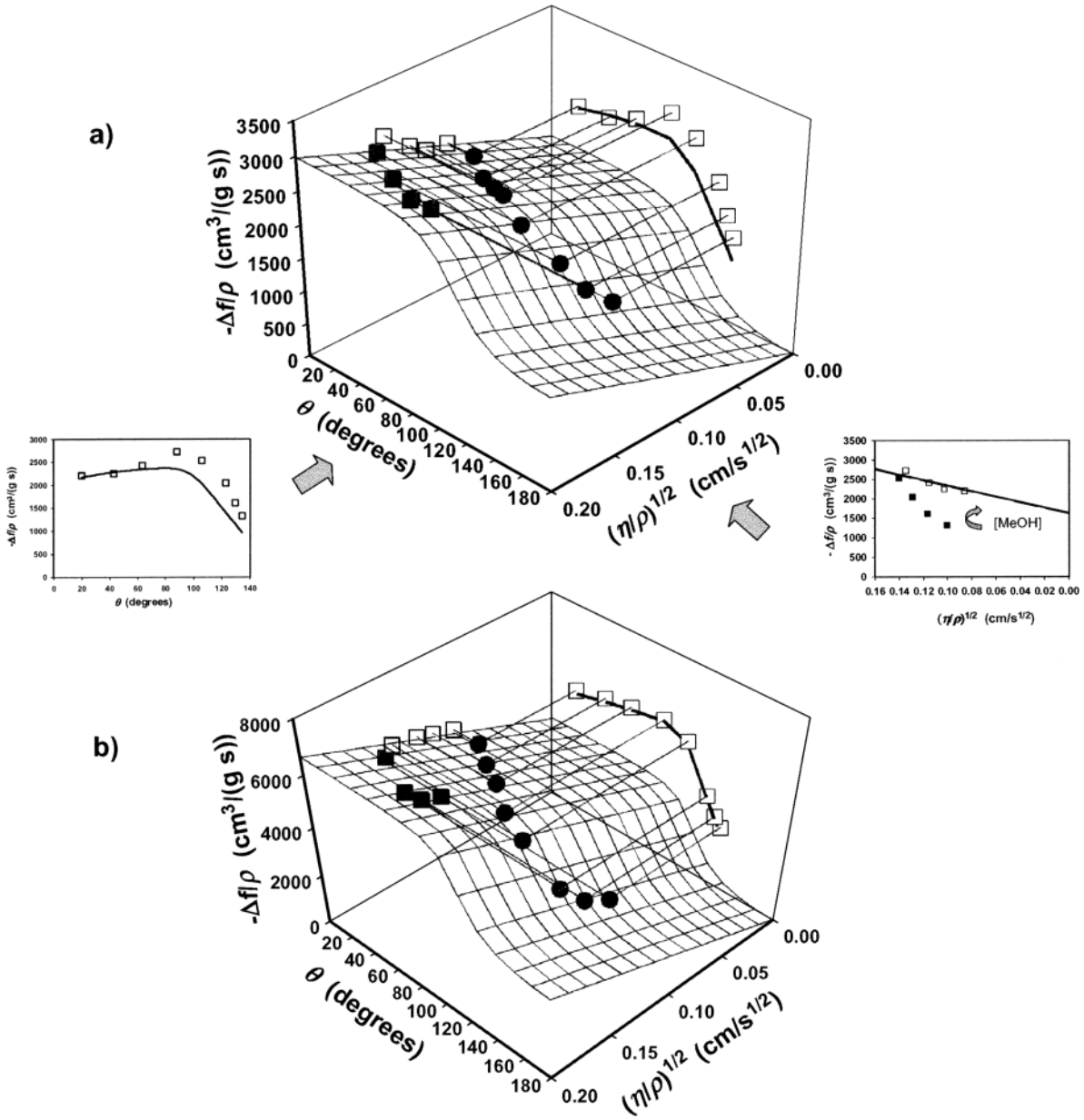

Figure 10. 3D plot of calculated response ($(-\Delta f/\rho)$ vs fluid properties ($(\eta/\rho)^{1/2}$) and contact angle (θ)) (surfaces using eq 6) and responses measured with MeOH/H_2O solutions[10] (●) at (a) 5 MHz and (b) 9 MHz. The boldface line is the calculated line from Figure 8. The other symbols are projections into their respective planes.

Figure 8 shows plots of $-\Delta f/\rho$ versus θ (analogous to the theoretical plots of Figure 5) for the data of Figure 7. The contact angles, reported by Yang et al.,[10] are *advancing* contact angles, measured with a Remy−Hart goniometer at room temperature. The lines show the response calculated from eq 6, based on the *incomplete wetting* model. We used the values of h obtained by fitting eq 5 to the data in Figure 7 (listed in Table 2, HDM-coated). The calculation was performed using contact angle (θ) and fluid property (η,ρ) values corresponding to the solutions used experimentally, connecting these with a smooth curve.

The ability of the incompletely wetted rough surface model to predict quantitatively the QCM response is gratifying. This success is accentuated by the recognition that, in making this calculation, we have *no adjustable parameters*. The only inputs are the fluid parameters (known separately) and the surface roughness derived from the fully wetted regime, i.e., by fitting eq 5 to the data as shown in Figure 7. In the latter case, the values are from within the same data set, but under conditions for which Figure 1b, rather than Figure 1c,d, represents the physical situation.

DISCUSSION

It would clearly be advantageous to have a generally applicable method, based on the QCM response, of diagnosing when the completely wetted rough surface or incompletely wetted rough surface models apply. Since Δf is a function of $(\eta/\rho)^{1/2}$ and of θ (see above), an obvious way of doing this is via a 3D representation in $[(\eta/\rho)^{1/2}, \theta, -\Delta f/\rho]$ space. In doing this, we point out that the formats of Figure 7 and Figure 8 to some extent give the misleading impression that (η/ρ) and θ can be varied totally independently. Although this may be possible in some circumstances (e.g., surfactant addition to a fluid) but not others (e.g.,

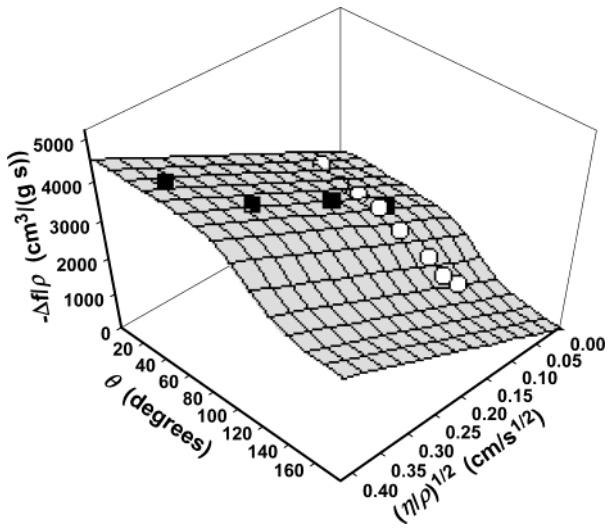

Figure 11. Normalized 3D plot (frequency shift ($-\Delta f/\rho$) vs fluid properties ($(\eta/\rho)^{1/2}$) and contact angle (θ)) of glycerol/water[11] data (■, $h = 192$ nm) and methanol/water[10] data (○, $h = 182$ nm) along with a calculated plane of similar h value ($h = 182$ nm).

the examples chosen here), it is nevertheless a valid and useful way to visualize the data.

Figure 9 shows a calculated three-dimensional representation of QCM response, $(-\Delta f/\rho)$ versus $(\eta/\rho)^{1/2}$ and θ. For $h = 0$, the response is a plane, independent of contact angle θ, and with a slope versus $(\eta/\rho)^{1/2}$ given by eq 5. For $h > 0$, we get surfaces that are *offset* at low θ values in proportion to h. The response diminishes with increasing θ, as the liquid becomes excluded from the corrugation. As $\theta \rightarrow 180°$, the offset surfaces converge to the $h = 0$ plane, consistent with the total elimination of trapped fluid from the surface features.

Visual inspection of Figure 9 shows that there are three regimes when $h > 0$. First, at low θ, the QCM response is confined to an inclined plane independent of θ but linearly dependent on h. This is the *fully wetted* corrugation regime of Figure 1b (response follows eq 5 for fixed value of h). Second, at high θ, the QCM response is confined to an inclined plane independent of θ and of h. This is the *fully de-wetted* corrugation regime of Figure 1d, in which the response is Kanazawa-like *even though the surface is not smooth*. Third, between these two θ-independent regimes, there is the *partially de-wetted* transition regime of Figure 1c in which increasing θ drives the de-wetting of the surface features.

Figure 10 shows the MeOH/H_2O data[10] for the HDM-coated QCM (from Figures 7 and 8) plotted versus $(\eta/\rho)^{1/2}$ and θ. As noted above, varying MeOH/H_2O concentration causes changes in fluid properties, $(\eta/\rho)^{1/2}$, and contact angle, θ. The surfaces in Figure 10 are calculated using the partial wetting model (eq 6) with the "HDM-coated" h values from Table 2. The data are seen to lie close to these calculated surfaces. The data of Figure 7 correspond to the projection of the 3-D points on the $(\eta/\rho)^{1/2} - (-\Delta f/\rho)$ plane, while the data of Figure 8 correspond to the projection of the same data on the $\theta - (-\Delta f/\rho)$ plane. The 3-D representation makes clear the decrease in response at higher θ values is caused by entry into the partially de-wetted regime in which fluid is excluded from roughness features.

Figure 11 shows both the glycerol/H_2O data[11] on a bare gold surface (Figure 6) and the MeOH/H_2O data[10] on an HDM-coated surface (Figure 7). The glycerol/H_2O (on bare gold surface) remains on the upper (mostly wetted) portion of the model surface, while the MeOH/H_2O data (on the HDM-coated surface) traverses both the wetted and partially wetted regions.

When Yang et al. originally published their MeOH/H_2O data,[10] they considered several possible explanations for the significant deviations in their data from the simple wetting model (eq 3). At low contact angle (θ), their measured Δf significantly exceeded the prediction, while at large θ, the response diminished significantly, as shown in Figure 8. They considered the possibility of contact angle-dependent trapping of fluid in surface roughness features (the model adopted here) but rejected this explanation. They considered the decrease in response observed at high θ to arise from the onset of "slip," i.e., a *discontinuity in particle velocity* across the solid/liquid interface.

In the present model, the shear mechanical displacement, which normally would be transmitted continuously across a solid/liquid interface, is interrupted by the presence of a gas bubble. While some authors would refer to this situation as "slip", we prefer to reserve this term for the situation when one has a discontinuity in particle displacement across a solid/liquid (or other) interface. This approach recognizes the importance of (inter) molecular forces at the interface. On the other hand, the gas bubble does interrupt (at a macroscopic level) the transmission of shear displacement from the solid to liquid, but since it has finite thickness, this does not really constitute slip in the strict continuum mechanical sense. We believe that the anomalous responses usually attributed to "slip" are in fact commonly not interfacial slip, but rather have a macroscopic origin and are caused by the presence of an intervening gas phase; this does not constitute "slip" in the strict sense.

It is a peculiarity of the QCM, due to its high operating frequency, that it probes a very thin liquid layer adjacent to the device surface (decay length ~250 nm in water). For this reason, to explain the response of the device requires one to examine phenomena on a length scale of tens of nanometers. At this level, a macroscopic model is inadequate and to label the process as "slip" misses the essential details of the problem.

The analysis presented here shows that a model based on classical wetting behavior on a rough surface is plausible and can adequately explain the observed deviations from the simple Kanazawa model. The only requirement is that one accepts the possibility of trapped gas/vapor occurring in those experiments; since (i) incomplete wetting corresponds to retreat of the liquid from parts of the solid and (ii) any liquid has a finite vapor pressure, this requirement would appear to be satisfied.

Our new model predicts the QCM response as a function of crystal properties (operating frequency and surface finish), fluid properties (η and ρ), and interfacial properties (θ). The literature data to which we have applied this new model encompass variations in all five parameters. In terms of the frequency response map of Figures 9 and 10, we have explored all but the completely de-wetted region. Our primary interests are in sensing in media (commonly aqueous) where the contact angle will not be extremely high. Thus, the completely wetted plane and the transition regime are the likely regime of operations. However, in more exotic media such as fluorocarbon solvents, or upon application of extremely hydrophobic surface treatments, the

completely de-wetted regime of Figure 1d may be encountered. Although beyond the scope of the present work, measurements on these more esoteric systems would allow completion of the testing of our model.

CONCLUSIONS

We have developed a model for QCM frequency responses incorporating roughness and de-wetting at the resonator/fluid interface. Within this model, we represent roughness as a stylized sinusoidal corrugation. Upon immersion of the resonator, liquid "sheets" across the surface, trapping gas in surface features. The interface between this trapped gas and the bulk liquid has a shape and area determined by a balance between internal pressure and surface tension forces. Application of classical arguments then allows one to determine the extent of liquid penetration ("wetting") of the surface corrugations. Although the model allows one to set the depth and periodicity of the corrugations independently, we have made specific calculations based on a depth/periodicity ratio ($A/\Lambda = 1/4$), which represents the case of a surface polished by monodisperse spherical abrasive. The outcome is that there are experimentally accessible regimes of parameter space in which the surface corrugations may be completely wetted, partially wetted, or completely de-wetted.

At low microscopic contact angle and small surface features, the surface is nearly or completely wetted; one can envisage this as surface tension forces causing crushing of the trapped gas bubble. The model then provides quantitative details of how increasing contact angle results in progressive de-wetting of the surface corrugations. The sharpness of the wetted-to-de-wetted transition, centered around a contact angle of $\sim$120°, increases as the surface feature size decreases: for surface features on the order of 100 nm, variation in contact angle of only 1−2° effects the complete transition. At high contact angle, wetting is so unfavorable as to result in completely liquid-free surface features, regardless of their size.

It is widely acknowledged that liquid trapped in surface features on a QCM resonator surface leads to an enhanced frequency shift, beyond that for viscously entrained fluid as predicted by the Kanazawa model. Thus, the foregoing considerations of corrugation wetting have allowed us to calculate a gravimetrically based contribution to the QCM frequency response for surface-entrapped liquid as a function of surface geometry, fluid density, and interfacial energetics. We have combined this with the Kanazawa result for a smooth surface to provide a model that incorporates the contributions of fluid both below and above the tops of surface features.

Application of the model to literature data shows how variations in fluid properties, for example in mixed solvents, can be accompanied by interfacial changes that result in simultaneous viscous and wetting effects. A visual means of identifying and representing these phenomena is presented. A prediction for highly lyophobic surfaces, in which there is complete exclusion of liquid from surface features, is that the QCM frequency response will be independent of surface finish.

ACKNOWLEDGMENT

Sandia is a multiprogram laboratory operated by Sandia Corp., a Lockheed Martin Company, for the United States Department of Energy's National Nuclear Security Administration under Contract DE-AC04-94AL85000. We thank the EPSRC for financial support (GR/N00968).

SUPPORTING INFORMATION AVAILABLE

Additional information as noted in text. This material is available free of charge via the Internet at http://pubs.acs.org.

Received for review July 10, 2003. Accepted November 18, 2003.

AC034777X